

Effect of short- and long-range scattering on the conductivity of graphene: Boltzmann approach vs tight-binding calculations

J. W. Kłos^{1,*} and I. V. Zozoulenko^{2,†}

¹*Surface Physics Division, Faculty of Physics, Adam Mickiewicz University, Umultowska 85, 61-614 Poznań, Poland*

²*Solid State Electronics, ITN, Linköping University, 601 74 Norrköping, Sweden*

(Received 22 June 2010; revised manuscript received 6 August 2010; published 27 August 2010)

We present a comparative study of the density dependence of the conductivity of graphene sheets calculated in the tight-binding (TB) Landauer approach and on the basis of the Boltzmann theory. The TB calculations are found to give the same density dependence of the conductivity, $\sigma^{\text{TB}} \sim n$, for short- and long-range Gaussian scatterers. In the case of short-range scattering the TB calculations are in agreement with the predictions of the Boltzmann theory going beyond the Born approximation but in qualitative and quantitative disagreement with the standard Boltzmann approach within the Born approximation, predicting $\sigma^{\text{Boltz}} = \text{const}$. Even for the long-range Gaussian potential in a parameter range corresponding to realistic systems the standard Boltzmann predictions are in quantitative and qualitative disagreement with the TB results. This questions the applicability of the standard Boltzmann approach within the Born approximation, commonly used for the interpretation of the results of experimental studies of the transport in graphene.

DOI: [10.1103/PhysRevB.82.081414](https://doi.org/10.1103/PhysRevB.82.081414)

PACS number(s): 73.63.Nm, 72.10.-d, 73.23.Ad

I. INTRODUCTION

Understanding factors that affect conductivity of graphene represents a fundamental task of great importance in view of possible application of graphene-based devices for electronics and optoelectronics. Currently, the majority of experimental measurements of conductivity σ in graphene^{1–8} is analyzed on the basis of the standard Boltzmann approach within the Born approximation predicting qualitative different results for short- and long-range impurity scattering^{9–13}

$$\sigma = \text{const} \quad (\text{short-range scattering}), \quad (1a)$$

$$\sigma \sim n \quad (\text{long-range scattering}), \quad (1b)$$

where n is the electron density. It has been recently argued by Stauber *et al.*¹³ that a standard way to examine the collision rate within the Born approximation (utilizing the unperturbed wave functions for a clean system) is not suitable for the case of short-range interaction such as vacancies, resonant impurities, cracks, etc. Going beyond the Born approximation, Stauber *et al.*¹³ and Katsnelson and Novoselov¹⁴ demonstrated that the short-range disorder, with the accuracy up to logarithmic corrections, leads to a linear density dependence similar to the one for the long-range potential,

$$\sigma = \frac{4e^2}{h} \frac{n}{n_i} (\ln \sqrt{\pi n R_0})^2, \quad (2)$$

where R_0 is the scatterer's radius and n_i is the impurity concentration. (Similar results have been also obtained by Ostrovsky *et al.*¹⁵) Apparently, this has important consequence for interpretation of the experimental results, as the linear density dependence of the conductivity is typically related to the long-range Coulomb impurities and deviations from this dependence is attributed to the short-range scattering.^{1–8} In contrast, Eq. (2) implies the short- and long-range scattering may lead to similar density dependencies of the conductivity. Indeed, Monteverde *et al.*¹⁶ have recently analyzed the experiment on the basis of Eq. (2) and arrived to the conclusion that strong neutral defects (as opposed to the long-range

Coulomb impurities) was the main scattering mechanism in graphene. The dominant role of neutral defects has been also recently outlined in Refs. 17 and 18.

The reliability of the above predictions Eqs. (1) and (2) can be established by testing them against “exact” Landauer-type quantum-mechanical numerical calculations for the conductivity based on the tight-binding (TB) (or Dirac) Hamiltonian for carriers in graphene.^{19–25} Recently, Adam *et al.*²⁴ compared the standard Boltzmann and the Landauer approaches for the case of a long-range Gaussian potential that varies smoothly on the scale of a lattice constant,

$$V_i = \sum_{i'=1}^{N_{\text{imp}}} U_{i'} \exp\left(-\frac{|\mathbf{r}_i - \mathbf{r}_{i'}|^2}{2\xi^2}\right), \quad (3)$$

where ξ can be interpreted as the effective screening length and the potential heights is assumed to be uniformly distributed in the range $U_i \in [-\delta, \delta]$. The conductivity obtained in the two approaches agrees quantitatively away from the Dirac point, which was interpreted as a proof of validity of both. According to Adam *et al.*,²⁴ the conductivity follows a density dependence $\sigma \sim n^{3/2}$. This, however, disagrees with all experimental observations reported so far^{1–8,16–18,26} and with previous Landauer-type numerical calculations^{21,20,24,25} demonstrating the linear or sublinear density dependence of the conductivity. Hence, a comparison between the Boltzmann and Landauer approaches still remains an open and an important issue.

The main purpose of the present study is to compare the exact Landauer TB conductivities with those given by the standard Boltzmann approach within the Born approximation as well as with those given by Eq. (2). As in the standard Boltzmann approach the density dependence is different for long- and short-range scatterers, one of our aims is to investigate whether the TB calculations also give different density dependencies for these scattering mechanisms. Finally, the Born approximation is valid for the case of weak scattering when the wave functions remains unperturbed. It is not, however, apparent that the condition of a weak scattering is sat-

ified in a parameter range typical for realistic systems. By comparing the exact TB calculations with those based on the predictions of the standard Boltzmann approach we test the applicability of the later to realistic systems.

II. THEORY

We calculate conductivity of the graphene sheets using the standard p -orbital nearest-neighbor tight-binding Hamiltonian for noninteracting electrons for zero temperature, $H = \sum_i V_i |i\rangle \langle i| - t \sum_{i,j} |i\rangle \langle j|$, with the hopping integral $t = 2.7$ eV.²⁷ We utilize a model for screened scattering centers of the Gaussian shape [Eq. (3)] commonly used in the literature.^{19,20,24,25} The correlator of the potential Eq. (3) has

the form,^{19,20,24} $\langle V_i V_j \rangle = \frac{K(\hbar v_F)^2}{2\pi\xi^2} \exp(-\frac{|r_i - r_j|^2}{2\xi^2})$, where the dimensionless impurity strength is described by the parameter $K \approx 40.5 n_{imp} (\delta/t)^2 (\xi/\sqrt{3}a)^4$ given by the screening length ξ , the potential strength δ , and the relative impurity concentration n_{imp} (a being the carbon-carbon distance and v_F is the Fermi velocity). For realistic graphene samples $K = 1 - 10$.^{19,20,24,25} In our calculations we use the screening length $1 \leq \xi/a \leq 8$, spanning the range between the short-range potential ($\xi = a$), and the long-range potential ($\xi = 8a$) that varies smoothly on the scale of a lattice constant. Note that we also performed calculations for the δ scattering, and the results obtained are, as expected, practically identical to those obtained for the case of the Gaussian disorder with $\xi = a$.

The conductance G and the electron density n are computed with the aid of the recursive Green's function technique.^{22,23,25} We assume that the semi-infinite leads are perfect graphene strips of the width W , and the device region is a rectangular graphene strip $W \times L$, where the impurity potential is defined. The zero-temperature conductance G is given by the Landauer formula $G = \frac{2e^2}{h} T$, where T is the total transmission coefficient between the leads. Then we calculated the conductivity $\sigma = \frac{L}{W} G$, the electron density $n = \int_0^{E_F} dE D(E)$, and the mean-free path (mfp) $\text{mfp} = \frac{h}{2e^2} \frac{\sigma}{\sqrt{\pi n}}$ as a function of the Fermi energy E_F . The density of states (DOS) $D(E)$ is computed by averaging the local DOS (LDOS) over the whole device area. The LDOS is given by the diagonal elements of the total Green's function.²² Because of computational limitations we study the strips with $L/W > 1$. [In most calculations we use $L = 368$ nm (3000 sites) and $L/W \approx 6$.] We, however, checked that the obtained results are insensitive to the aspect ratio L/W as soon as $L/W > 1$.

The results of the tight-binding calculations are compared to the predictions obtained within the standard Boltzmann approach within the Born approximation for the scattering potential Eq. (3). The conductivity of graphene sheet is given by⁹⁻¹⁴ $\sigma = e^2 \tau D(E_F) \frac{v_F^2}{2}$, where the DOS $D(E_F) = 2E_F / (\pi \hbar^2 v_F^2)$, the dispersion relation $E = \hbar v_F k$, and $k = \sqrt{\pi n}$ with $v_F = \frac{3at}{2\hbar}$ being the Fermi velocity. The scattering rate within the Born approximation reads $\tau^{-1} = \frac{2\pi}{\hbar} D(E) \frac{1}{4} \int_0^\pi \frac{d\theta}{\pi} \frac{1 - \cos^2 \theta}{2} |U_q|^2$, where U_q is the Fourier transform of the scattering potential, $q = |\mathbf{k} - \mathbf{k}'| = 2k \sin \frac{\theta}{2}$, where θ is the angle between the initial and final states \mathbf{k} and \mathbf{k}' . Using the Wiener-Kitchine theorem for the correlator, we

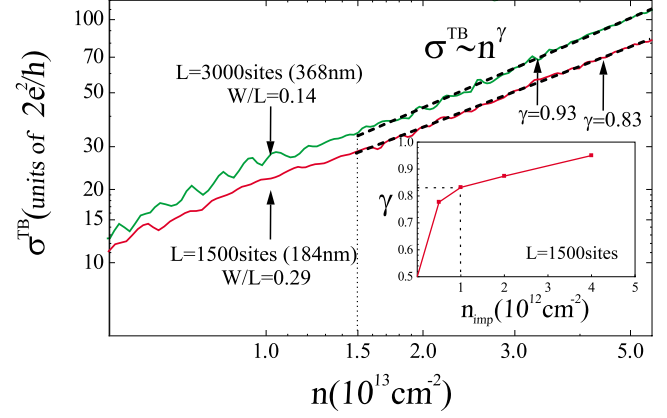


FIG. 1. (Color online) (a) The conductivity vs the electron density for two representative graphene strips with different lengths $L = 3000$ and 1500 sites for the case of the short-range scattering ($\xi = a$) with $n_{imp} = 10^{12}$ cm $^{-2}$. Each curve is averaged over eight impurity configurations. The impurity strength $\delta = 0.86t$. The inset shows the dependence $\gamma = \gamma(n_{imp})$.

obtain the Fourier transform of the Gaussian potential, $|U_q|^2 = K(\hbar v_F)^2 \exp(-q^2 \xi^2/4)$, which leads to the expression for the conductivity,^{12,24}

$$\sigma^{Boltz} = \frac{4e^2}{h} \frac{\pi n \xi^2 e^{\pi n \xi^2}}{K I_1(\pi n \xi^2)} \sim \text{const}, \quad \pi n \xi^2 \ll 1, \quad (4)$$

$$\sim n^{3/2}, \quad \pi n \xi^2 \gg 1,$$

where I_1 is the modified Bessel function.

III. RESULTS AND DISCUSSIONS

The Boltzmann predictions for the density dependence of the conductivity are valid in the diffusive transport regime when the mfp is larger than a system size. Let us therefore first discuss a transition from the ballistic to diffusive regime focusing on the short-range scattering, $\xi = a$. In a purely ballistic regime (no impurity scattering) the conductivity follows the density dependence $\sigma \sim n^\gamma$ with $\gamma = \frac{1}{2}$.²⁵ It has been demonstrated for the case of the long-range Gaussian scatterers that with the increase in the system size the exponent γ gradually increases from its ballistic value reaching the value $\gamma = 1$ in the diffusive regime.²⁵ Figure 1 shows the dependence $\sigma = \sigma(n)$ for the case of the short-range scattering calculated within the TB approach. The conductivity shows the same behavior as for the case of the long-range scattering²⁵ with γ increasing from $\frac{1}{2}$ in the ballistic regime to $\gamma = 1$ in the diffusive regime as the size of the system or the impurity concentration increases. This obtained density dependence in the diffusive regime ($\gamma = 1$) is in a stark contrast with the standard Boltzmann predictions for the δ -impurity scattering, Eq. (1a), when σ is expected to be density independent ($\gamma = 0$).

A more detailed comparison between the TB and Boltzmann calculations for the short-range scatterers for different impurity strengths δ is presented in Figs. 2(a) and 2(b). As expected, for very weak scattering ($\delta \lesssim 0.5t$) the transport is in the ballistic regime with $\gamma \approx 1/2$. This is fully consistent with the calculated mfp which is comparable to the largest

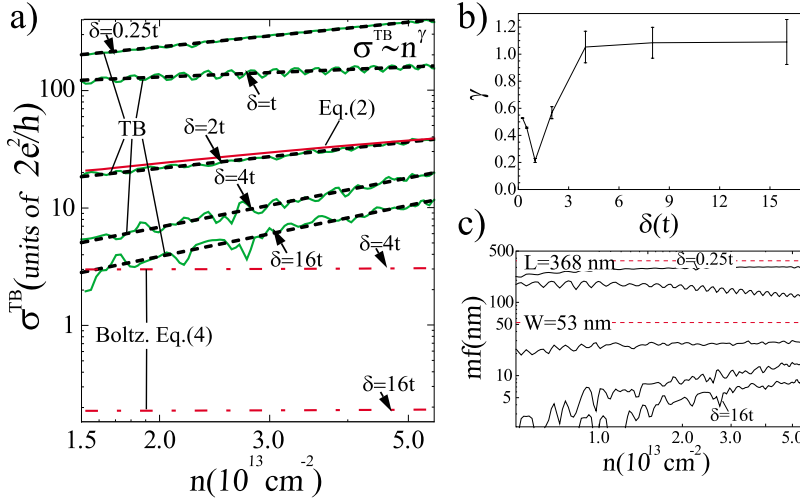


FIG. 2. (Color online) (a) The conductivity of the graphene sheets vs electron density for the short-range Gaussian potential with $\xi=a$ for different potential strength δ . Each curve is averaged over eight impurity configurations. Straight dashed lines show fitting $\sigma \sim n^\gamma$. Red solid and dotted-dashed lines show predictions based, respectively, on Eqs. (2) and (4). (b) The dependence $\gamma = \gamma(\delta)$. (c) The mfp vs the electron density n . $n_{imp} = 8 \times 10^{12} \text{ cm}^{-2}$, $L=3000$ sites (368 nm), $W/L=0.14$.

dimension of the system L , see Fig. 2(c). For the case of strong scattering ($\delta \geq 2.5t$) the system is in the diffusive transport regime when the calculated mfp is smaller than the smallest dimension of the system W . In this regime the exponent γ saturates to 1, see Fig. 2(b). Figure 2(a) also shows the conductivity calculated on the basis of the standard Boltzmann approach, Eq. (4), as well as given by Eq. (2). The Boltzmann theory predicts that $\gamma=0$ which is in qualitative disagreement with the numerically calculated exponent $\gamma \approx 1$. Boltzmann predictions are also quantitatively different from the tight-binding calculations with $\sigma^{Boltz} \ll \sigma^{TB}$ (note the logarithmic scale of the figure). At the same time, we find that the TB calculations are in a good qualitative and even reasonable good quantitative agreement with Eq. (2) predicting quasilinear density dependence of the conductivity. Why does the standard Boltzmann approach fail to describe the conductivity of the system at hand? Following Stauber *et al.*,¹³ we believe this is because the scattering rate τ in the standard Boltzmann approach is calculated in the Born approximation, with unperturbed clean-graphene wave functions. Apparently, this approximation is applicable in the case of weak perturbations but cannot be applied for strong scattering potential. In contrast, the approach proposed by Stauber *et al.* uses wave functions for a hard-wall barrier, appropriate in the case of strong scattering.

Let us finally compare the tight-binding and Boltzmann calculations for the long-range Gaussian scatterers with $\xi=8a$ for different impurity strengths, see Fig. 3. As for the case of the short-range scatterers the TB calculations exhibit the ballistic behavior ($mfp \approx L$) with $\gamma=1/2$ for weak scattering and the diffusive behavior ($mfp \leq W$) with $\gamma \approx 1$ for the strong scattering. Again, the result obtained in the diffusive regime, $\gamma \approx 1$, is qualitatively different from the corresponding Boltzmann prediction. Indeed, for the latter case the exponent γ is poorly defined because for the considered density interval $\pi n \xi^2 \approx 1$ which, according to Eq. (4), corresponds to the transition regime between two asymptotes $\sigma^{Boltz} = \text{const}$ and $\sigma^{Boltz} \sim n^{3/2}$. Besides, the Boltzmann and the tight-binding calculations disagree even quantitatively with $\sigma^{Boltz} \ll \sigma^{TB}$. [Note the logarithmic scale of Fig. 3(a).]

The opposite limit $\pi n \xi^2 \gg 1$ (when $\sigma \sim n^{3/2}$) was considered by Adam *et al.*²⁴ who found a good qualitative and quantitative agreement between the Landauer-type and the Boltzmann calculations. This regime (in contrast to the regime $\pi n \xi^2 \leq 1$ considered here) corresponds to high electron energies and smooth potential (with large ξ) when the scattering is weak and the Boltzmann theory within the Born approximation is therefore justified. However, the density dependence predicted by Eq. (4), $\sigma^{Boltz} \sim n^{3/2}$, has never been observed in any experiment. In contrast, the dependence

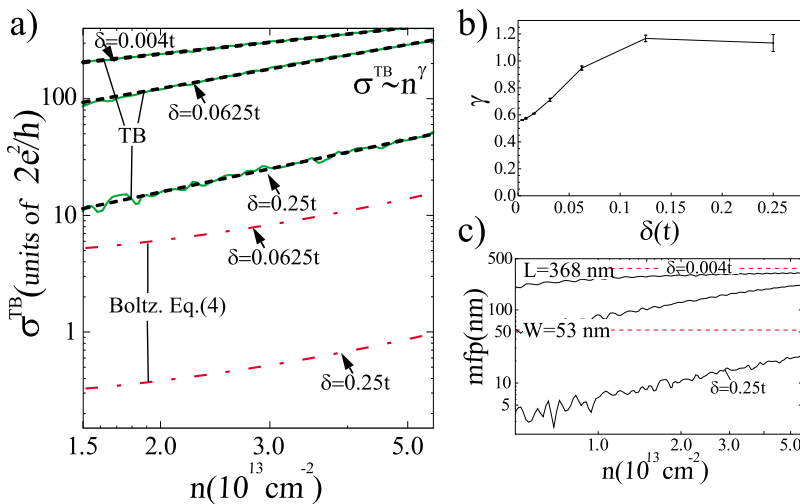


FIG. 3. (Color online) (a) The conductivity of the graphene sheets vs electron density for the long-range Gaussian potential with $\xi=8a$ for different potential strength δ . Each curve is averaged over eight impurity configurations. Straight lines show fitting $\sigma \sim n^\gamma$. Dashed lines show predictions based on Eq. (4). (b) The dependence $\gamma = \gamma(\delta)$. (c) The mfp vs the electron density n . Parameters of the graphene sheet are the same as in Fig. 2.

$\sigma^{TB} \sim n$, obtained in the TB calculations for the regime $\pi n \xi^2 \lesssim 1$ considered here, is in agreement with the majority of experimental findings. We regard this as a strong indication that the regime appropriate for realistic graphene samples is $\pi n \xi^2 \ll 1$. As demonstrated here, in this parameter range the results obtained in the standard Born approximation disagree both quantitatively and qualitatively with those obtained by the exact TB calculations. This therefore questions the validity of the standard Boltzmann predictions within the Born approximation for realistic graphene sheets.

Let us finally discuss the transition regime between the ballistic and diffusive behavior when $W < \text{mfp} < L$. For the short-range scatterers the exponent γ shows a pronounced minimum dropping to $\gamma \approx 0.2$ for $\delta \approx t$, whereas for the long-range scatterers γ increases monotonically from 0.5 to 1, cf. Figs. 2(b) and 3(b). We are not aware of any theories addressing this transition regime corresponding to the quasiballistic transport. We speculate, however, that this peculiar behavior might be related to the corresponding Boltzmann results predicting $\sigma^{\text{Boltz}} = \text{const}$ and $\sigma^{\text{Boltz}} = \sigma^{\text{Boltz}}(n)$ for the short- and long-range scatterers, respectively, [see dotted-dashed curves in Figs. 2(a) and 3(a) corresponding to Eq. (4)]. It is worth to emphasize that while in the diffusive regime σ^{TB} shows the same linear density dependence for the long- and short-range scatterers, in the quasiballistic regime the corresponding σ^{TB} are different. Our findings suggest that quasiballistic transport regime can be used to distinguish

between the effects of short- and long-range Coulomb scattering.

IV. CONCLUSIONS

(i) In the diffusive transport regime the TB calculations give the same linear density dependence of the conductivity, $\sigma^{TB} \sim n$, for both short- and long-range Gaussian scatterers.

(ii) In the case of short-range potential the obtained linear dependence is in quantitative and qualitative disagreement with the standard Boltzmann predictions within the Born approximation, Eqs. (1a) and (4) but in agreement with the predictions going beyond the Born approximation, Eq. (2).

(iii) Even for the long-range Gaussian potential the standard Boltzmann predictions Eq. (4) are in quantitative and qualitative disagreement with the TB results in the parameter range corresponding to realistic systems ($\pi n \xi^2 \lesssim 1$ regime). This questions the applicability of the predictions based on the standard Boltzmann theory for conductivity in graphene which are widely used for interpretation of experimental data.

ACKNOWLEDGMENTS

Discussions with N. M. R. Peres, T. Heinzl, H. Xu, A. Shylau, and F. Vasko are greatly appreciated. I.V.Z. acknowledges support from the Swedish Research Council (VR).

*klos@amu.edu.pl

†igor.zozoulenko@itn.liu.se

- ¹S. V. Morozov, K. S. Novoselov, M. I. Katsnelson, F. Schedin, D. C. Elias, J. A. Jaszczak, and A. K. Geim, *Phys. Rev. Lett.* **100**, 016602 (2008).
- ²Y.-W. Tan, Y. Zhang, K. Bolotin, Y. Zhao, S. Adam, E. H. Hwang, S. Das Sarma, H. L. Stormer, and P. Kim, *Phys. Rev. Lett.* **99**, 246803 (2007).
- ³K. I. Bolotin, K. J. Sikes, Z. Jiang, M. Klima, G. Fudenberg, J. Hone, P. Kim, and H. L. Stormer, *Solid State Commun.* **146**, 351 (2008).
- ⁴K. I. Bolotin, K. J. Sikes, J. Hone, H. L. Stormer, and P. Kim, *Phys. Rev. Lett.* **101**, 096802 (2008).
- ⁵W. Zhu, V. Perebeinos, M. Freitag, and Ph. Avouris, *Phys. Rev. B* **80**, 235402 (2009).
- ⁶C. Jang, S. Adam, J.-H. Chen, E. D. Williams, S. Das Sarma, and M. S. Fuhrer, *Phys. Rev. Lett.* **101**, 146805 (2008).
- ⁷B. Huard, N. Stander, J. A. Sulpizio, and D. Goldhaber-Gordon, *Phys. Rev. B* **78**, 121402 (2008).
- ⁸X. Hong, K. Zou, and J. Zhu, *Phys. Rev. B* **80**, 241415 (2009).
- ⁹K. Nomura and A. H. MacDonald, *Phys. Rev. Lett.* **96**, 256602 (2006); **98**, 076602 (2007).
- ¹⁰T. Ando, *J. Phys. Soc. Jpn.* **75**, 074716 (2006).
- ¹¹E. H. Hwang, S. Adam, and S. Das Sarma, *Phys. Rev. Lett.* **98**, 186806 (2007).
- ¹²F. T. Vasko and V. Ryzhii, *Phys. Rev. B* **76**, 233404 (2007).
- ¹³T. Stauber, N. M. R. Peres, and F. Guinea, *Phys. Rev. B* **76**, 205423 (2007).
- ¹⁴M. I. Katsnelson and K. S. Novoselov, *Solid State Commun.* **143**, 3 (2007).
- ¹⁵P. M. Ostrovsky, I. V. Gornyi, and A. D. Mirlin, *Phys. Rev. B* **74**, 235443 (2006).
- ¹⁶M. Monteverde, C. Ojeda-Aristizabal, R. Weil, K. Bennaceur, M. Ferrier, S. Guéron, C. Glattli, H. Bouchiat, J. N. Fuchs, and D. L. Maslov, *Phys. Rev. Lett.* **104**, 126801 (2010).
- ¹⁷L. A. Ponomarenko, R. Yang, T. M. Mohiuddin, M. I. Katsnelson, K. S. Novoselov, S. V. Morozov, A. A. Zhukov, F. Schedin, E. W. Hill, and A. K. Geim, *Phys. Rev. Lett.* **102**, 206603 (2009).
- ¹⁸Z. Ni, L. Ponomarenko, R. Nair, R. Yang, S. Anissimova, I. Grigorieva, F. Schedin, Z. Shen, E. Hill, K. Novoselov, and A. Geim, [arXiv:1003.0202](https://arxiv.org/abs/1003.0202) (unpublished).
- ¹⁹J. H. Bardarson, J. Tworzydło, P. W. Brouwer, and C. W. J. Beenakker, *Phys. Rev. Lett.* **99**, 106801 (2007).
- ²⁰C. H. Lewenkopf, E. R. Mucciolo, and A. H. Castro Neto, *Phys. Rev. B* **77**, 081410(R) (2008).
- ²¹J. P. Robinson, H. Schomerus, L. Oroszlány, and V. I. Fal'ko, *Phys. Rev. Lett.* **101**, 196803 (2008).
- ²²H. Xu, T. Heinzl, M. Evaldsson, and I. V. Zozoulenko, *Phys. Rev. B* **77**, 245401 (2008).
- ²³H. Xu, T. Heinzl, and I. V. Zozoulenko, *Phys. Rev. B* **80**, 045308 (2009).
- ²⁴S. Adam, P. W. Brouwer, and S. Das Sarma, *Phys. Rev. B* **79**, 201404(R) (2009).
- ²⁵J. W. Klos, A. A. Shylau, I. V. Zozoulenko, H. Xu, and T. Heinzl, *Phys. Rev. B* **80**, 245432 (2009).
- ²⁶X. Du, I. Skachko, A. Barker, and E. Y. Andrei, *Nat. Nanotechnol.* **3**, 491 (2008).
- ²⁷A. H. Castro Neto, F. Guinea, N. M. R. Peres, K. S. Novoselov, and A. K. Geim, *Rev. Mod. Phys.* **81**, 109 (2009).